NOTES AND CORRESPONDENCE

The Average Behavior of Large-Scale Westward-traveling Disturbances Evident in the Southern Hemisphere Geopotential Heights

P. SPETH AND W. MAY

Institute for Geophysics and Meteorology, University of Cologne, Cologne, Germany

R. A. MADDEN

National Center for Atmospheric Research, Boulder, Colorado*

18 March 1991 and 21 June 1991

1. Introduction

Evidence for large-scale, westward-traveling disturbances has been provided by space–time spectral analyses of geopotential heights. In particular, Speth and Madden (1983) report relative maxima in westward-propagating, zonal wavenumber one (wave-1) variance of Northern Hemisphere geopotential height data in the 13–32-day period range. Based on Southern Hemisphere data, Mechoso and Hartmann (1982) isolated westward-propagating wave-1 variance in the 13–17-day period range.

Figure 1, taken from Barbulescu (1990), is presented to further illustrate this evidence. The space–time spectra of Fig. 1 are for wave 1 during the solstice seasons, and are based on European Centre for Medium Range Weather Forecasts (ECMWF) analyses from 1979 through 1987. The method used to determine Fig. 1 is that described by Hayashi (1977) and Speth and Madden (1983). Relative maxima in westward-propagating variance are evident near 16-day and slightly longer periods at high latitudes of both hemispheres. Barbulescu found similar results for the equinox seasons.

These space–time spectral results are generally thought to reflect the presence of waves similar to the theoretically predicted Rossby normal modes of an isothermal atmosphere at rest. Each normal mode possesses a distinct frequency and horizontal structure, although frequencies can blur together and horizontal structures can change somewhat in the presence of realistic winds (e.g., Salby 1981). Their vertical structures are like that of a Lamb wave modified by dissipation (Salby 1980). We might expect that an individual disturbance could be separated into a number of different modes, both symmetric and antisymmetric, about the equator. The idea that individual disturbances may sometimes be comprised of a number of distinct modes has been supported by observational work. This support comes from projecting data onto theoretically predicted structures of the normal modes (Hough functions) and determining if the propagation speeds of the projections are consistent with the theory (e.g., Ahlquist 1982; Lindzen et al. 1984). A second approach is to bandpass filter data in time to isolate a propagation speed and compare the horizontal structures of any evident moving disturbances with theoretical expectations (Hirooka and Hirota 1985; Venne 1989).

In spite of the possibility that some traveling disturbances may result from the superposition of a number of quasi-normal modes, we think it is useful to try to answer the question "*What is the average structure of the phenomena responsible for the westward-propagating variance evident in the 13–32-day period range of space–time spectral analyses such as those shown in Fig. 1?*", and to do this without assuming that they result from such a superposition. In an earlier paper, we tried to answer that question for the space–time spectra of middle and high northern latitudes (Madden and Speth 1989, MS hereafter). That effort was based on a minimum of space and time filtering in order to avoid "building in" results a priori. We found that the disturbances were predominantly wave 1 in longitudinal scale and for about half of the year global in that they were discernible in the Southern Hemisphere.

This paper follows MS closely, but seeks to define the average structure of disturbances responsible for the westward-propagating variance of geopotential height evident in the space–time spectra from middle and high *southern* latitudes. In MS, we used data from 60°N to determine episodes of westward propagation,

* The National Center for Atmospheric Research is sponsored by the National Science Foundation.

Corresponding author address: Dr. Roland A. Madden, NCAR, P.O. Box 3000, Boulder, CO 80307.

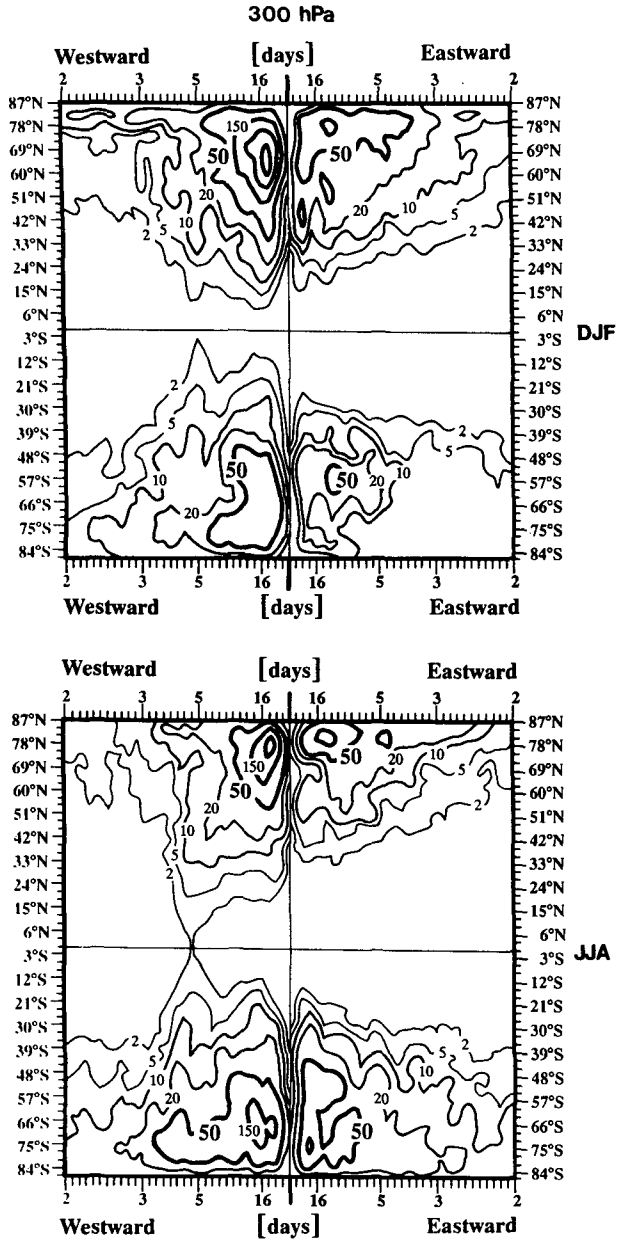

FIG. 1. Space–time spectra of geopotential height for wave 1 in gpm^2 at 300 hPa and at different latitudes for DJF (top) and JJA (bottom). Periods are in days with westward-(eastward-) propagating variance indicated to the left (right). [Taken from Barbulescu (1990).]

while here we use data from 60°S. Also in MS, we demonstrated that the dominant longitudinal scale of the disturbances responsible for the aforementioned space–time spectral results at 60°N was wave 1 at nearly all latitudes. Here, for easy comparison, we concentrate only on wave 1.

2. Data and method

The data used in this study were derived from the ECMWF operational analyses for the period June 1980 through May 1987. References that describe the analysis system are contained in MS. Daily, 0000 UTC analyses of geopotential heights were Fourier transformed along 59 latitude circles at 3° intervals from 87°N to 87°S. The zonal means and the first eight wavenumbers from 13 pressure levels between 1000 hPa and 30 hPa were retained.

From Hovmoeller diagrams for wave 1 at 60°S and 250 hPa we identified episodes of westward propagation for the four seasons. In constructing these diagrams a smoothed, seasonally varying, forced wave 1 was first removed. The forced component was determined by ensemble averaging, over all years, the wave-1 sine and cosine coefficients for 1 January, 2 January, etc. These ensemble averages were then smoothed by including only the annual, the semiannual, the third, and half the amplitude of the fourth harmonic. The selection rules were the same as in MS:

1) Westward propagation had to be evident on the Hovmoeller diagrams for more than one-half the circumference of the earth.

2) The period of a complete revolution had to be eight or more days. No other time filtering was done except that the seasonally varying mean was subtracted as mentioned above.

3) For estimating the average structure, data were composited according to season. Seasons were December–January–February (DJF), March–April–May (MAM), June–July–August (JJA), and September–October–November (SON). For tabulating the durations and periods of episodes, each episode was assigned to the season in which westward propagation was first identified.

From diagrams as in Figs. 3 and 4 (to follow) we determined the presence and phase of westward-propagating disturbances of wave 1 at 16 longitude points (22.5 degree separation) along 60°S. For each day when westward propagation was evident, we assigned the date to one of 16 phase categories according to the longitudes of zero lines. Composites were then determined for each phase by averaging the zonal mean and all eight zonal wavenumbers separately according to the assigned phase category and subtracting the appropriate seasonal average. In the following section we discuss the results for the wave-1 components of the composites.

3. Results

a. Durations and periods of episodes of westward propagation

Table 1 gives for each season the duration of individual episodes, the number of complete circuits of the globe during the episode, the resulting average period in days, and the date and phase when the episode began. In Table A of the Appendix, we relate the episodes

TABLE 1. The number of continuous days of westward propagation of wave 1 at 60°S and 250 hPa during each identified episode (Duration), the corresponding number of times the wave makes a complete circuit (Circuits), and the average period (Period) during the episode. The data judged to be the beginning of the episode (Month/day and Year) and the phase of the ridge in wave 1 on that date (Phase) is also indicated. Positive values are degrees east and negative values degrees west. The right-hand column contains the total number of days when westward propagation was identified during the eight (seven for JJA) years, the total number of circuits, and the resulting average period in days.

						JJA							
Duration	7	44	12	26	7	11	18	24	18	14			181
Circuits	0.81	2.44	0.94	1.13	0.50	0.88	0.63	1.56	0.81	0.88			10.5
Period	9	18	13	23	14	13	29	15	22	16			17
Month/day	0712	0306	0624	0726	0708	0814	0605	0804	0530	0707			
Year	1980	1981	1982	1982	1983	1983	1984	1985	1986	1986			
Phase	292.5	180	90	247.5	292.5	135	90	270	337.5	202.5			
						SON							
Duration	16	14	8	10	22	18	23	11	17				139
Circuits	1.69	1.31	0.50	0.69	1.69	1.38	1.06	0.94	1.75				11.1
Period	9	11	16	15	13	13	22	12	10				13
Month/day	0910	0929	1025	1103	0826	1003	0918	0829	0925				
Year	1982	1982	1982	1983	1984	1984	1985	1986	1986				
Phase	225	0	180	315	225	202.5	135	135	292.5				
						DJF							
Duration	10	15	16	35	13	10							99
Circuits	0.50	0.69	1.19	1.94	0.81	0.56							5.7
Period	20	22	13	18	16	18							17
Month/day	0210	1214	0216	1126	0122	0211							
Year	1981	1981	1982	1984	1985	1986							
Phase	112.5	112.5	22.5	67.5	180	202.5							
						MAM							
Duration	15	9	11	19	12	11	21	15	25	21	9	13	170
Circuits	1.31	0.56	0.50	1.31	1.13	0.88	1.63	0.88	1.88	1.69	0.75	0.94	12.6
Period	11	16	22	14	11	13	13	17	13	12	12	14	13
Month/day	0331	0520	0403	0416	0415	0526	0323	0427	0308	0501	0328	0422	
Year	1981	1981	1982	1982	1983	1983	1984	1985	1986	1986	1987	1987	
Phase	337.5	202.5	337.5	292.5	0	45	135	247.5	67.5	112.5	270	45	

determined in this paper for the Southern Hemisphere with those for the Northern Hemisphere from MS.

Grand totals are contained in the rightmost column. Westward-propagating waves were present about 28% (JJA), 22% (SON), 16% (DJF), and 26% (MAM) of the time. For comparison with the corresponding seasons for the Northern Hemisphere (MS), these percents are 38% (DJF), 34% (MAM), 35% (JJA), and 27% (SON). In each case, except possibly in local fall, westward disturbances are evident more frequently in the Northern Hemisphere. It is interesting to note that, for example, during DJF identified disturbances are less than half as frequent in the Southern Hemisphere.

The average duration of an episode, given by dividing the total number of days when westward propagation was identified by the number of episodes, is similar in each hemisphere for the equinox seasons but about 25% longer in the Northern Hemisphere during the solstice seasons. The average durations for the Southern Hemisphere from Table 1 are 18 (JJA), 15 (SON), 16 (DJF), and 14 (MAM) days. For the Northern Hemisphere, from Table 1 in MS, they are 23 (DJF), 15 (MAM), 22 (JJA), and 15 (SON) days. The longest duration from Table 1 here is 44 days (JJA) while from Table 1 in MS it is 72 days (DJF). The average period for the Southern Hemisphere ranges from 13 (SON) to 17 (DJF and JJA) days. In the Northern Hemisphere we found a range of 16 (MAM and JJA) to 20 (DJF) days.

b. *Composite structure of wave-1 westward-propagating disturbances*

In a manner similar to MS, we now look in detail at the global structure of the wave-1 component of the composites. The average amplitude and average phase with respect to 500 hPa and 60°S is determined over 16 phase categories, as in Eqs. (3) and (4) of MS. The results are contained in Fig. 2 in which the contour lines represent the average amplitude in geopotential meters. Arrowheads are plotted only at pressure levels

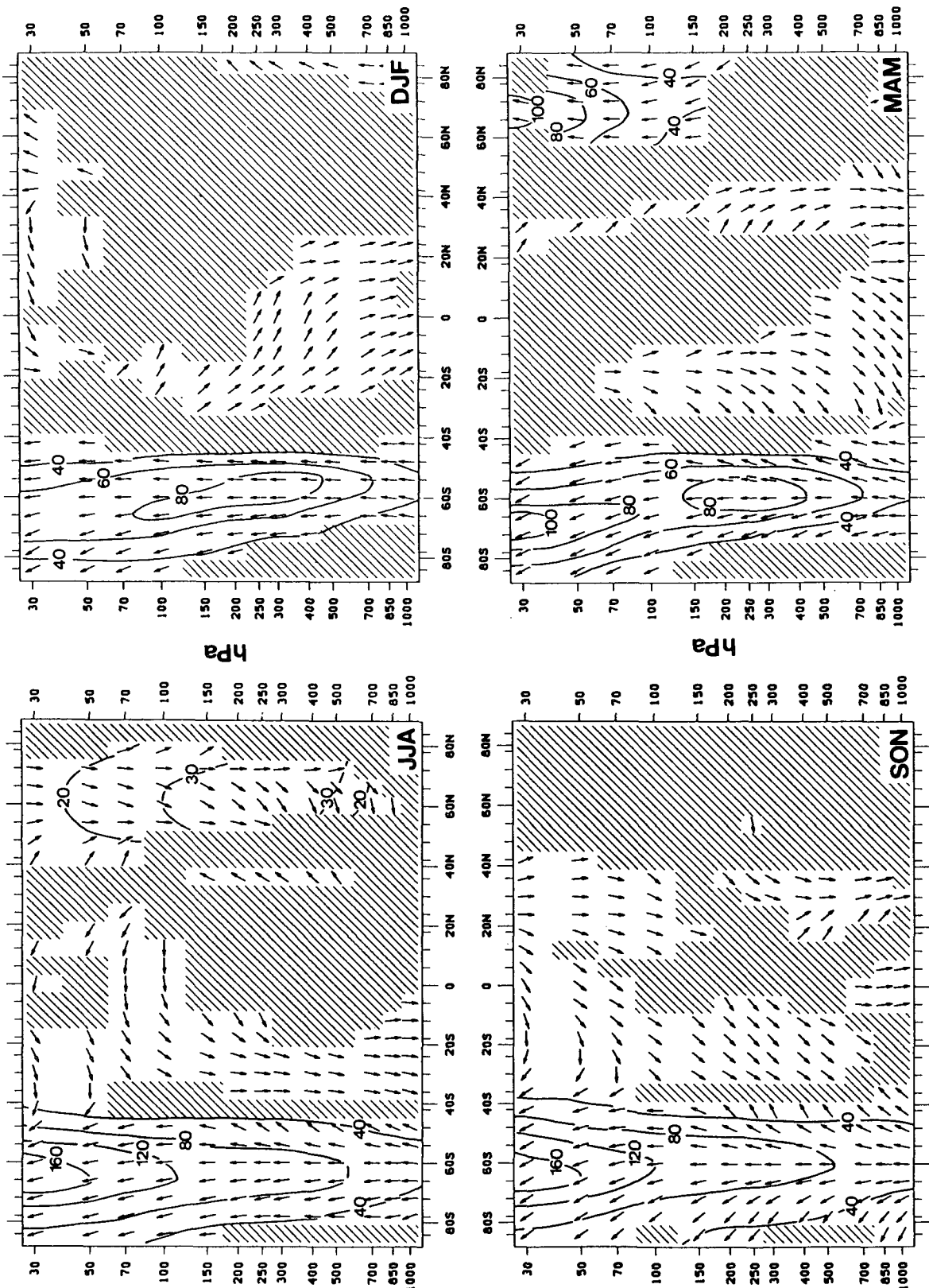

FIG. 2. Structure of the zonal wave-1 component of the composite for the months indicated by the initials in the lower right of each panel. Arrowheads represent pressure levels and latitudes where westward propagation was evident. Their orientation indicates the phase between the wave at the given level and latitude and that at 500 hPa and 60°S. Arrows pointing up mean that the wave at that point is, when averaged over the 16-phase categories, in phase with that at 500 hPa and 60°S. Arrows pointing to the left or down mean that it is to the west of or out of phase with that at 500 hPa and 60°S. Shaded regions are regions of minimum coherence (≤ 0.25) with the wave at 500 hPa and 60°S. Contours are in geopotential meters.

and latitudes where visual inspection of time–longitude sections of the composites clearly indicated westward propagation of their wave-1 component. The orientation of the arrowheads reflects the phase relationship between the wave at a given pressure level and latitude and that at a reference (500 hPa, 60°S). Arrows pointing upward (downward) mean that the waves at the two locations are in phase (out of phase). Arrows pointing to the left (right) mean that the wave at that point is west (east) of that at the reference point. Additionally, we computed the coherence between the wave at the reference and all other points. In MS we determined through a Monte Carlo simulation that a coherence exceeding 0.25 was rare (1% occurrence) given a true coherence of zero. The shaded regions in Fig. 2 indicate where the computed coherencies were less than or equal to 0.25.

From Fig. 2 we see that the wave is present nearly everywhere poleward of 40°S for all seasons. It is approximately in phase with the reference point. During SON there is, however, a 90 degree horizontal phase shift oriented northeast (40°S)–southwest (80°S) throughout the troposphere. This indicates a poleward momentum transport during this season. There is little or no vertical slope throughout the troposphere at these latitudes, but a slight westward slope exists in the stratosphere. This latter feature indicates a poleward heat transport.

In all seasons evidence for the waves is reduced between 30° and 40°S and may reflect a nodal region. Within the troposphere the tropical region tends to be out of phase with middle and polar southern latitudes. During SON in the stratosphere, the wave changes phases by 180 degrees from 40°S to 40°N through a gradual westward slope. During JJA the wave is nearly out of phase between high southern and high northern latitudes, while during MAM in the stratosphere it is in phase between those latitudes. Poleward of 40°S where the amplitudes are large, their vertical growth is monotonic as that of a Lamb wave within the troposphere. But there appear to be seasonal differences of the vertical structure within the stratosphere. During JJA and SON the amplitude increases above the tropopause with height, but in DJF it decreases. Results are intermediate between these two cases for MAM. This seasonal change in the vertical growth of the waves may reflect a seasonal change in wave evanescence in response to strongest lower stratospheric westerlies in JJA and SON, weaker ones in MAM, and easterlies in DJF (Randel 1987).

Comparing Fig. 2 here with Figs. 7–10 in MS reveals many common features. There are, however, important

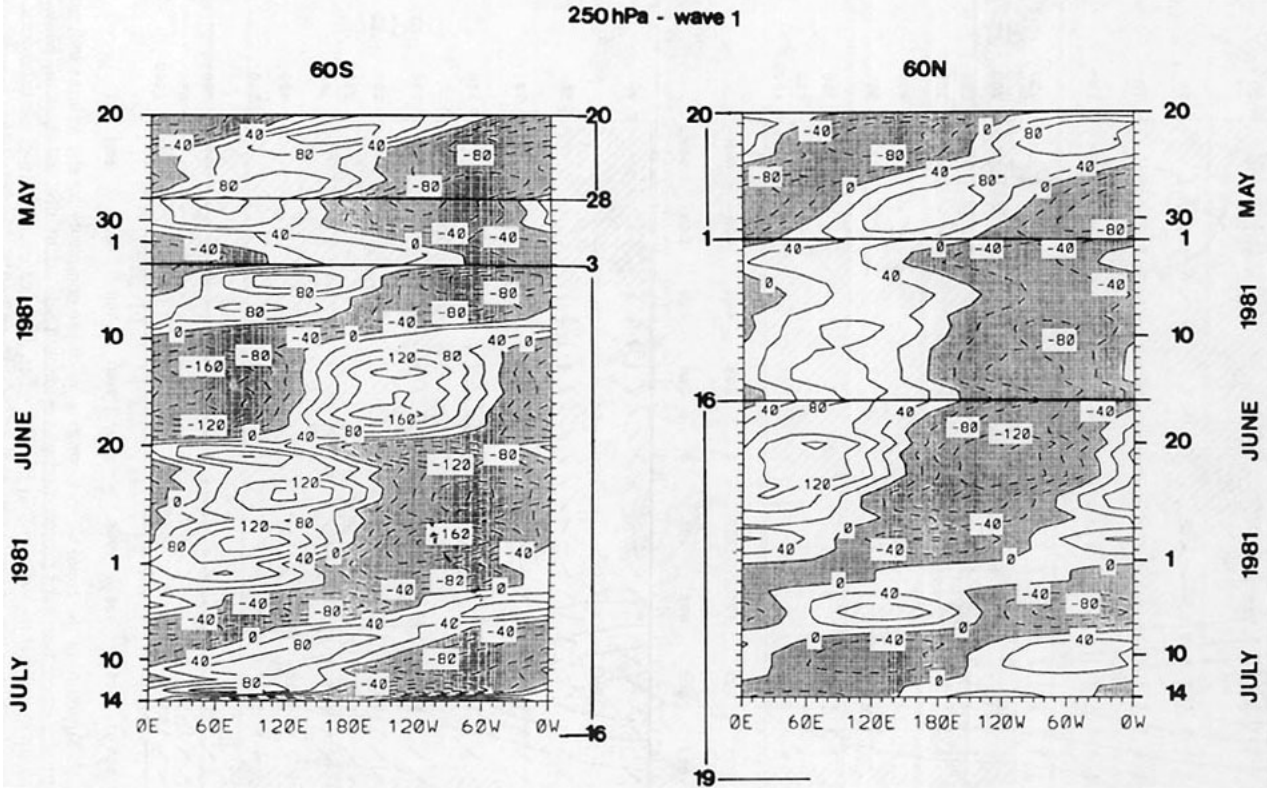

FIG. 3. Time–longitude (Hovmoeller) diagrams of daily values of wave 1 at 250 hPa for 60°S (left) and for 60°N (right) for the period 20 May through 14 July 1981. A smooth seasonally varying wave 1 has been subtracted from each. Units are geopotential meters. Episodes of westward propagation are indicated by the vertical lines in the margins.

differences. Here we find regular westward propagation and coherence at more levels and latitudes than in MS. When constructing composites based on Northern Hemispheric data, as in MS, little evidence of the waves south of 20°N during MAM and JJA was found. Here, the reverse is not the case. Interestingly enough, Fig. 2 for JJA indicates a coherent wave in high northern latitudes out of phase with that of high southern latitudes. In contrast, during MAM the wave is coherent and in phase between these latitudes.

In the case where the wave appears to be global in the sense that it extends between middle and high latitudes of both hemispheres, we might expect that composites based on Northern or Southern Hemispheric dates would be similar. Comparing Fig. 2 here with the corresponding Figs. 7–10 in MS shows that this is not the case. In this regard, it turned out that more than half of the individual episodes of westward propagation selected based on the Southern Hemispheric Hovmoeller diagrams had no corresponding episodes evident in the Northern Hemispheric Hovmoeller diagrams used in MS. Dates of all selected episodes in this paper and from MS are listed in the Appendix for easy comparison.

c. Individual episodes of traveling wave 1

Hovmoeller diagrams for wave 1 at 60°S and 250 hPa are shown in Figs. 3 and 4. They include the episodes beginning 20 May 1981, 3 June 1981, 2 May 1986, and 30 May 1986, which are contained in Table A. Also shown in Figs. 3 and 4 are Hovmoeller diagrams for wave 1 at 60°N and 250 hPa that were prepared for but not published in MS. The latter diagrams include episodes that began on 20 May 1981, 16 June 1981, and 6 May 1986. These episodes were selected for display because they contain both in- and out-of-phase cases.

The episode originating about 20 May 1981 is clearly out of phase between 60°S and 60°N (Fig. 3). The episode beginning 3 June 1981 at 60°S has no obvious traveling counterpart at 60°N until about 16 June when the Southern Hemisphere wave appears to trail that in the North by about one-fourth of a cycle. Again, through the first half of July 1981 the wave is out of phase between the hemispheres. In Fig. 4, there is only a short time from 6 to 17 June 1986 when there are traveling waves clearly evident at both 60°S and 60°N. During that time they are in phase.

This latter case notwithstanding, the composite results of Fig. 2 suggest that it is the nearly out-of-phase cases that dominate during June–July–August.

4. Summary

Here we have followed the procedures used in our earlier paper (MS) to define the three-dimensional structure of disturbances responsible for relative maxima in the westward space–time spectra of zonal wave-

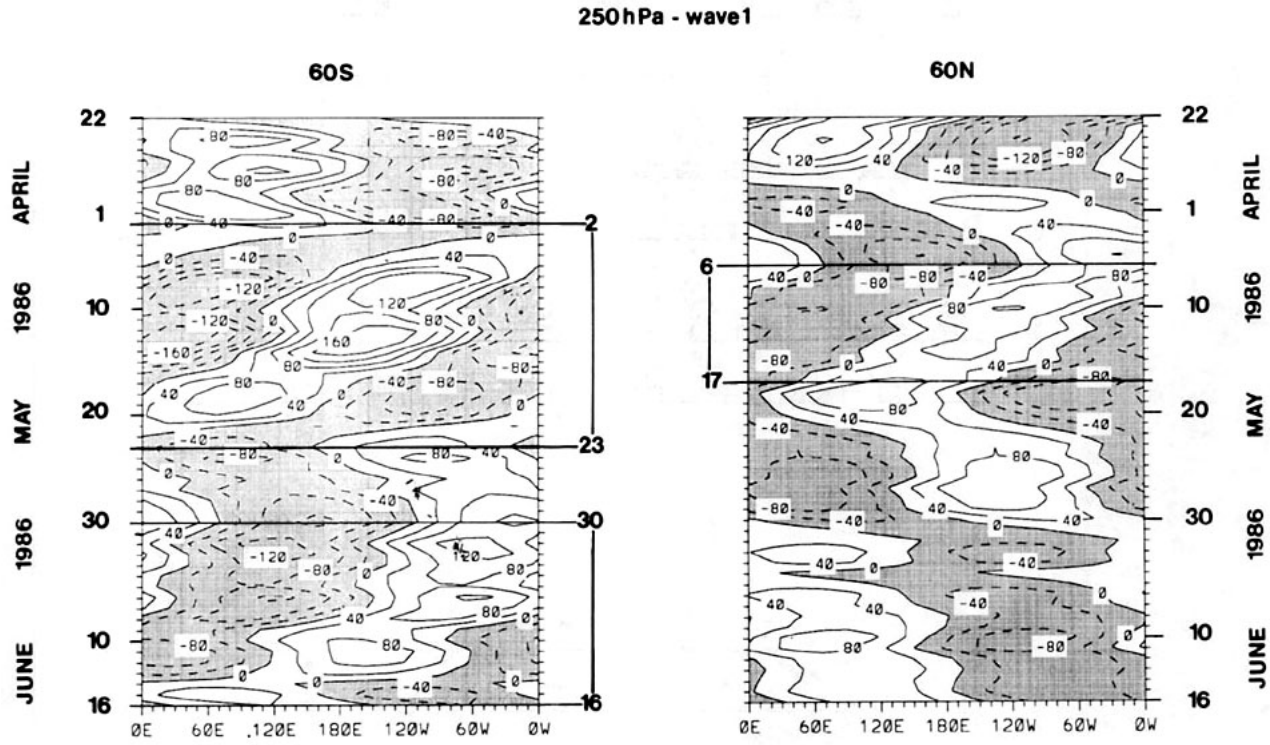

FIG. 4. As in Fig. 3 but for the period 22 April through 16 June 1986.

Appendix: Table A

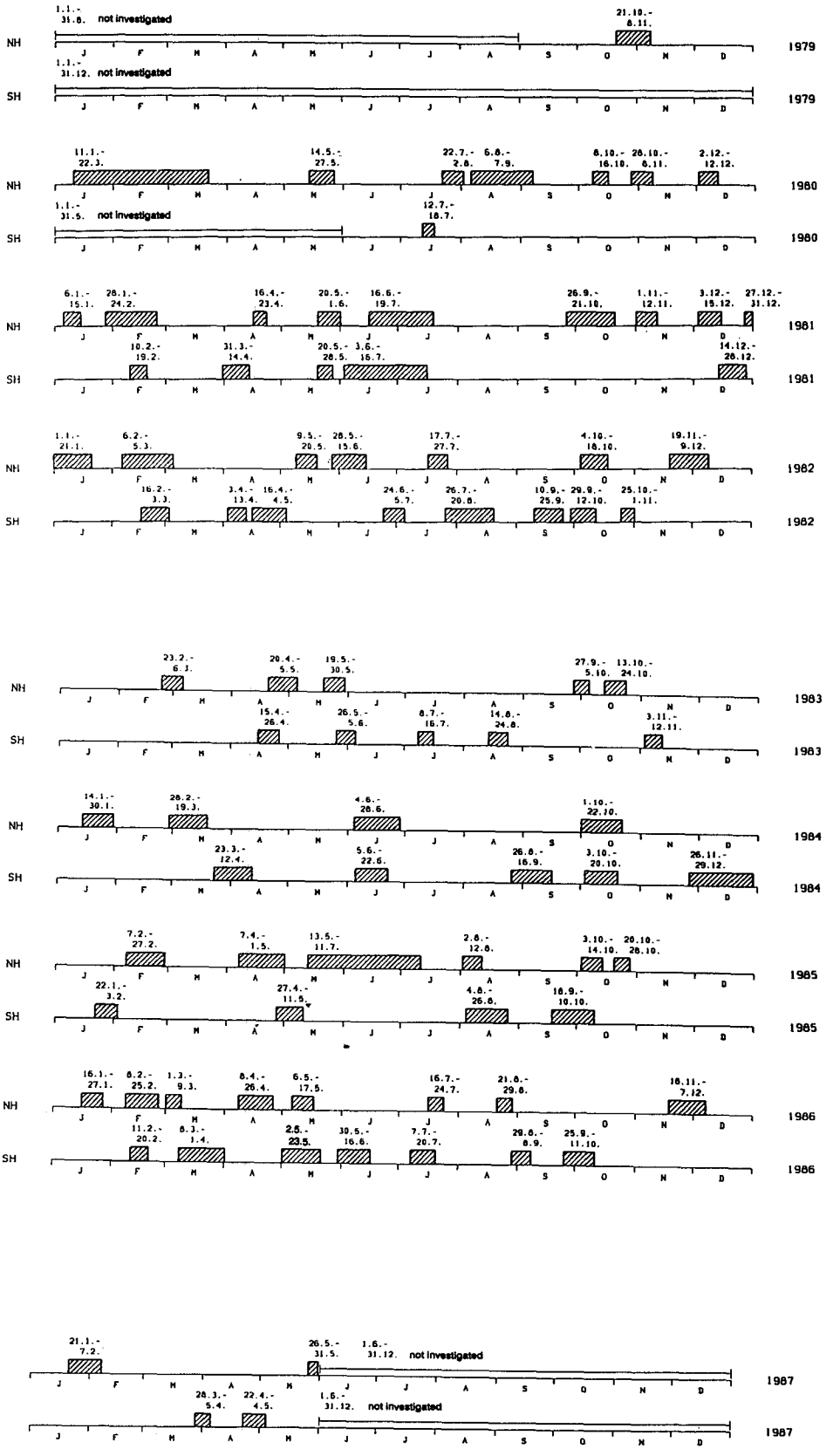

TABLE A. Calendar of westward-propagating episodes.

number one near 16 days. In MS, we concentrated on peaks evident at 250 hPa and 60°N, while here we concentrated on those evident at 250 hPa and 60°S. Westward propagation was evident at 60°S from approximately 16% (DJF) to 28% (JJA) of the time, and average periods ranged from 13 (SON) to 17 (DJF and JJA) days. Similar results reported in MS for 60°N indicated westward propagation evident from about 27% (SON) to 38% (DJF) of the time. Average periods at 60°N were from 16 (MAM and JJA) to 20 (DJF) days. The disturbances tend to be more prevalent and reflect slightly longer periods at 60°N than at 60°S. Average durations of episodes may be slightly longer at 60°N (15 days during MAM and SON to 23 days during DJF) than at 60°S (14 days during MAM to 18 days during JJA).

We might have expected that, if we are dealing with disturbances forced in the winter hemisphere, the JJA composite determined here would be nearly a mirror image of the DJF composite determined in MS. To some extent that is true; however, in Fig. 2 we have, on average, an out-of-phase relationship between 60°S and 60°N while in Fig. 7 of MS that relationship is more nearly in phase. Also, the DJF composite amplitudes in the stratosphere over northern latitudes from MS are approximately 50% larger than the corresponding JJA values from Fig. 2 here.

The regular occurrence of these wave disturbances implies that they are Rossby normal modes. Because these normal modes are global, it was at first surprising that there were relatively few episodes of westward propagation evident at 60°S with contemporaneous westward propagation at 60°N (see Appendix). Further consideration suggests that this is what should be expected, especially if forcing is confined to a single hemisphere: for instance, if we assume that an episode is forced by changing wind speeds over a mountain range as simulated by Garcia and Geisler (1981). If this forcing is confined to the winter hemisphere, then all normal modes, upon whose spatial structures the forcing projects and whose time scales overlap to some degree the time scale of the forcing, will be excited. Initially, their sum would be nonzero only in the region of the forcing, and only after time would dispersion of modes allow for evidence of the disturbance in other areas. We have seen that the average duration of an episode is two to three weeks. This is not enough time for the first antisymmetric mode (10-day wave, Hirooka and Hirota 1985) and the second symmetric mode (16-day wave, Madden 1978), which would initially cancel each other far from the forcing region, to separate enough to be identified there. We plan to investigate these speculations further by projecting data onto normal-mode structures during the episodes determined here and in MS.

APPENDIX

In the calendar (Table A) we indicate the time when episodes of westward propagation were evident at 250 hPa at 60°N (indicated by NH, taken from MS) and at 60°S (indicated by SH). Beginning and ending dates are indicated by day and month. Hirooka and Hirota (1989) have presented a parallel calendar for westward-propagating disturbances of distinct frequencies at 1 mb for 1980 through 1985. Since our method cannot distinguish between different meridional modes and theirs can as a result of time filtering, a complete comparison of these two calendars will have to await the projection of our data onto normal-mode structures.

REFERENCES

Ahlquist, J. E., 1982: Normal-mode global Rossby waves: Theory and observations. *J. Atmos. Sci.*, **39,** 193–202.

Barbulescu, M., 1990: Atmosphärische Eigenschwingungen in Modell und Beobachtungen. Mitteilungen aus dem Institut für Geophysik und Meteorologie der Universität zu Köln, **73,** 186 pp.

Garcia, R. R., and J. E. Geisler, 1981: Stochastic forcing of small-amplitude oscillations in the stratosphere. *J. Atmos. Sci.*, **38,** 2187–2197.

Hayashi, Y., 1977: On the coherence between progressive and retrogressive waves and a partition of space-time power spectra into standing and traveling parts. *J. Appl. Meteor.*, **16,** 368–373.

Hirooka, T., and I. Hirota, 1985: Normal mode Rossby waves observed in the upper stratosphere. Part II: Second antisymmetric modes of zonal wave numbers 1 and 2. *J. Atmos. Sci.*, **42,** 536–548.

——, and ——, 1989: Further evidence of normal mode Rossby waves. *Pure Appl. Geophys.*, **130,** 277–289.

Lindzen, R. S., D. M. Straus, and B. Katz, 1984: An observational study of large-scale atmospheric Rossby waves during FGGE. *J. Atmos. Sci.*, **41,** 1320–1335.

Madden, R. A., 1978: Further evidence of traveling planetary waves. *J. Atmos. Sci.*, **35,** 1605–1618.

——, and P. Speth, 1989: The average behavior of large-scale westward traveling disturbances evident in the Northern Hemisphere geopotential heights. *J. Atmos. Sci.*, **46,** 3225–3239.

Mechoso, C. R., and D. L. Hartmann, 1982: An observational study of traveling planetary waves in the Southern Hemisphere. *J. Atmos. Sci.*, **39,** 1921–1935.

Randel, W. J., 1987: Global atmospheric circulation statistics, 1000–1 mb. NCAR Tech. Note, NCAR/TN-295+STR, 245 pp.

Salby, M. L., 1980: Rossby normal modes in nonuniform background configurations. Part II: Equinox and solstice conditions. *J. Atmos. Sci.*, **38,** 1827–1840.

——, 1981: The influence of realistic dissipation on standing normal structures. *J. Atmos. Sci.*, **37,** 2186–2199.

Speth, P., and R. A. Madden, 1983: Space-time spectral analyses of Northern Hemisphere geopotential heights. *J. Atmos. Sci.*, **40,** 1086–1100.

Venne, D. E., 1989: Normal-mode Rossby waves observed in the wavenumber 1–5 geopotential fields of the stratosphere and troposphere. *J. Atmos. Sci.*, **46,** 1042–1056.